**IEEE Robotics and Automation Letters (RA-L) paper, presented at ICRA 2026, Vienna, Austria. Cite as RA-L paper.**

# Equilibrium State for a Tailless Flapping Wing Micro Air Vehicle in Forward Flight

Ernesto Sanchez-Laulhe[1], Guido C.H.E de Croon[2], *Member, IEEE* and Anibal Ollero[3], *Fellow, IEEE*

***Abstract*—Flapping wing Micro Air Vehicles (FWMAVs) hold great potential for real-world applications but are currently still hard to model. In this article, a simplified analysis of the equilibrium state of a tailless FWMAV in forward flight is presented. The definition of the equilibrium state complements previous dynamic and stability analysis, adding new information about the flight behavior of FWMAVs. A new aerodynamic decoupled model has been used for the analysis, considering separately the thrust force generated by the flapping movement and the lift and drag caused by the forward velocity. The aerodynamic forces are included in a dynamic model of the FWMAV, and the equilibrium state is derived. The formulation obtained is explicit in terms of the pitch actuator deflection, thus allowing its use for control corrections, and provides an estimation of the flight velocity. The thrust needed to maintain height is also formulated, demonstrating that forward flight is more efficient than hovering. The results are validated experimentally for the pitch angle, showing good agreement with the analytical results. Then, the dynamics of the FWMAV are simulated, comparing the results with experiments where the FWMAV goes from hovering to a specific pitch reference while maintaining its height. Additional simulations are performed with basic control considerations, showing how considering the equilibrium state for a feed-forward control significantly improves the flight behavior compared to PI and PID controllers, reducing the convergence time.**

***Index Terms*—Biologically-Inspired Robots; Aerial Systems: Mechanics and Control; Dynamics**

## I. Introduction

Flying animals show a series of flight characteristics in different scales which make them a source of inspiration. Birds have high efficiency for long-range flight, whereas insects or hummingbirds have the ability to hover in stable positions and show great agility in closed spaces. FWMAVs draw inspiration from animal flyers, using their flapping wing as their propulsive system to maintain flight [1]–[4]. These vehicles achieve great performance with unique characteristics. For example, they are safer for the environment than traditional multirotors, as well as less noisy, due to the lack of propellers. These advantages are mentioned in [5]. . However, tailless FWMAVs are also inherently unstable, using their wings for flight control and stabilization.

Manuscript received: June, 17th, 2025; Revised September, 19th, 2025; Accepted October, 25th, 2025.

This paper was recommended for publication by Editor Xinyu Liu upon evaluation of the Associate Editor and Reviewers' comments. This work was supported by the University of Malaga and the Advanced Grant of the European Research Council GRIFFIN.

[1]E. Sanchez-Laulhe is with the Fluid Mechanics group, University of Malaga, Malaga, Spain ernesto.slaulhe@uma.es

[2]G.C.H.E de Croon is with the Micro Air Vehicles Lab., TU Delft, Delft, Netherlands g.c.h.e.decroon@tudelft.nl

[3]A. Ollero is with the GRVC Robotics Lab., University of Seville, Seville, Spain aollero@us.es

Digital Object Identifier (DOI): see top of this page.



Fig. 1. FWMAV during flight.

Performing controlled flights in FWMAVs is a challenge. Flapping wing propulsion exploits unsteady aerodynamics to generate thrust. These unsteady aerodynamics depend on complex fluid-structure interactions and are not yet fully understood. Modeling the aerodynamics and arising forces is still an active area of research, using both analytical and CFD models [6].

Preliminary work showed a basic maneuver control for stable hovering and maneuver, but the precision was limited as they neglected the flight dynamics [7]. With on-board feedback for the attitude, PD controllers can perform well for simple maneuvers, once the information about the pitch and roll moments generated by the actuators is obtained [8]. Other works have also proven controllability for hovering maneuvers or reduced pitch and roll angles [9].

However, understanding the flight dynamics is basic for the development of more advanced controllers and the optimization of the design [10], [11]. Taking advantage of the fact that the flapping frequencies in FWMAVs are normally of a higher order than the characteristic dynamic frequencies, most models use rigid body assumptions, considering just the average terms for the flapping forces and neglecting the oscillations due to the flapping itself [12]. Although certain studies also consider a more complex approach with multi-body dynamics [13], the results are similar in terms of characteristic dynamic times, identifying some additional complex behaviors leading to additional instabilities. However, the complexity of these multi-body systems is much higher and the added information can be neglected for practical purposes in control and dynamic response, thus simplifying the analysis. This is the approach followed here.

The first studies for flapping wing dynamics come from

**IEEE Robotics and Automation Letters (RA-L) paper, presented at ICRA 2026, Vienna, Austria. Cite as RA-L paper.**

biology and the analysis of the flight of insects and are focused mainly on the stability and dynamic response, proving the instability of open loop flight [14]. Additional analyses have shown that tailless FWMAVs are also unstable in open loop flight [15]. Instability has motivated further study of the dynamic responses to the controller, to achieve a stable hovering [16].

Although most works are focused on hovering, mainly in the dynamic response and stability and damping of perturbations, other maneuvers have also been analyzed in the literature. For instance, a take off maneuver has been analyzed, finding different stability modes compared to hovering [17]. The work in [18] is focused on the stability of descending flight, even though the same analysis shows the instability for the opposite climbing flight. Forward flight dynamic response has been also studied [19], achieving a stable control in forward flight [20].

For this work, we propose a different approach, presenting a basic dynamic model to analyze the equilibrium state of FWMAV. The analysis provides an explicit formulation for pitch and velocity in horizontal forward flight. The formulation of the equilibrium state enables better feedforward control, counting less on other control approaches, e.g. an integrator. A simplified aerodynamic decoupled model has been used to formulate the aerodynamic forces during the forward flight. This model considers separately the thrust generated with the flapping movement and the forces generated by the wing with the incoming velocity neglecting the effects of the flapping.

Thus, the contribution of this work is a new formulation for the equilibrium state of FWMAVs in forward flight, based on rigid body dynamics commonly used for these aerial platforms. The solution of the pitch has been experimentally validated, showing a good agreement with our theoretical results. Results obtained can be used for improving the performance of the controllers, but also for optimizing the design to obtain the desired range of pitch and velocity for the FWMAV in forward flight.

This letter is structured as follows: in section II we develop the aerodynamics and the dynamic model. Section III contains the analysis of the equilibrium state. The validation of the equilibrium pitch angle and velocity is shown in section IV, as well as simulations for the dynamic response, also validated, and basic control simulations to show the potential of the proposed analysis to improve flight behavior. Then, some final remarks are provided in section V.

## II. Flight Model

The analysis developed here is focused on the tailless FWMAV designed in TU Delft, the Delfly Nimble [4] or its bigger size commercial version, the Flapper Nimble+. Those prototypes, propelled by flapping wings in X configuration, include 4 control variables for independent control of pitch, yaw, roll and thrust. However, the formulation is general for any FWMAV as long as the assumptions made here can be applied to them. Those assumptions, used to formulate simple equations to predict the movement of the FWMAV, are the following:

- The flapping frequency of the flapping movement is much bigger than the characteristic frequencies of the system. Assuming this hypothesis, the oscillation of the forces during the flapping cycle can be neglected and the average terms are used instead. Furthermore, the X-wing configuration ensures that moments from the wing along the flapping stroke direction are canceled. Namely, one wing moves up at the same time that another identical wing moves down, canceling reaction forces and moments.
- The aerodynamic forces, thrust, lift, and drag ($T$,$L$,$D$), are centered in a fixed position on the wing surface. With this hypothesis, we can assume that the sums of the forces of each pair of wings are centered in the same position during the flapping cycle, being modified just when the pitch actuator moves. In addition, the aerodynamic center positions for both pairs of wings are symmetrical with respect to the longitudinal plane.
- The effects of moving the wings forward and backward with the pitch actuation on the center of mass can be neglected due to their relatively light weight (less than 10% of the total weight). Furthermore, the effects of the moving parts on the dynamic behavior of the FWMAV can also be neglected, so that it can be taken as a rigid body.
- There are only two control actions with effects on longitudinal flight, the deflection of the pitch actuation, provided by a servomotor, and the frequency of the flapping movement $f$, provided by the motors. The deflection of the pitch actuation, the angle of the servo, displaces the neutral angle of the flapping cycle, leading to a change in position for the center of pressure. The displacement of the center of pressure generates a moment by deviating the thrust force from the alignment with the center of gravity (for more details, see Ref. [4]). For succinctness, we will refer to pitch actuation as the change in the position of the center of pressure, defined by $l_d$. The rest of the control actions affect only the lateral dynamics and are actuated here only to maintain constant yaw and no roll in the FWMAV.

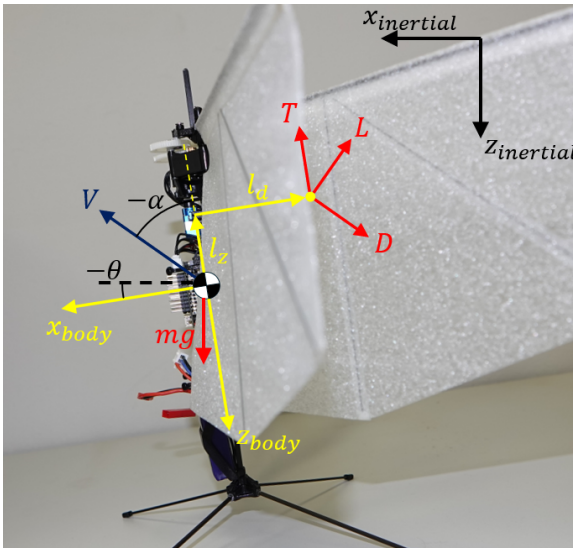


Fig. 2. Scheme of variables and forces over the FWMAV.

**IEEE Robotics and Automation Letters (RA-L) paper, presented at ICRA 2026, Vienna, Austria. Cite as RA-L paper.**

### A. Dynamic model

The previous assumptions allow us to use the rigid body equations for the FWMAV. We can obtain the dynamics of the FWMAV using the Newton-Euler formulation in the body frame. The aerodynamic forces, identified as $X$ and $Z$ for the forces in both axes and $M$ for the moment, are defined later in section II-B. The resulting dynamic equations are

$$m\dot{u} = -m\dot{\theta}w - mg\sin(\theta) + X, \tag{1}$$

$$m\dot{w} = m\dot{\theta}u + mg\cos(\theta) + Z, \tag{2}$$

$$I\ddot{\theta} = M, \tag{3}$$

with the state variables being the velocities in the body frame, $u$ and $w$, and the pitch angle, $\theta$. The mass $m$ and the inertia $I$ are characteristic parameters of the FWMAV, and $g$ is the gravity acceleration. The angle of attack, as well as the absolute velocity, can be computed from the velocities in the body frame:

$$\alpha = \arctan\left(\frac{-u}{-w}\right); \quad V = \sqrt{u^2 + w^2}. \tag{4}$$

Note that velocities are defined with respect to air. In the presence of wind, these velocities are not the same as the ground velocity. Note also that, as well as the formulation is written with the velocities in the body frame as the state variables, we could also use the absolute velocity and the angle of attack alternatively. In fact, for the equilibrium state analysis in section III, the total velocity is a state variable to compute and the angle of attack is fixed with the pitch angle. Note that, given equations (1)-(3), the characteristic dynamic time is approximately $t_c \sim u_c/g\theta_c \sim 1$ s, with the characteristic velocity of order $u_c \sim 1\,\mathrm{m/s}$ and the characteristic pitch angle $\theta_c \sim 0.1$, estimated for low pitch angle movements. This characteristic time is much longer than the one associated with the flapping frequency ($f \sim 10\,\mathrm{Hz}$), and therefore the flapping oscillations can be neglected as proposed in the initial assumptions. Note also that for higher pitch angles, the aerodynamic model proposed here is expected to fail, as commented in subsection II-B.

A scheme of the forces and variables can be found in figure 2. We see how the deflection $l_d$ moves the center of pressure, creating an aerodynamic moment on the center of gravity. In this case, the pitch angle and the angle of attack are negative, so the lift is also negative as will be defined in subsection II-B. However, the formulation of the aerodynamic forces is needed to quantify the relation between that deflection and the dynamic response of the FWMAV.

### B. Aerodynamic forces

For hovering, the aerodynamic forces in a FWMAV are well-defined. The flapping movement provides an instantaneous incoming velocity on the wing, generating forces perpendicular and opposite to the velocity (lift and drag). The design with two pairs of flapping wings cancels the reaction force/moment that would otherwise rock the body. Anyway, when the flapping frequency is high enough, the forces are considered only with average terms, generating an average force, usually defined as a thrust force. The force direction is in the vertical axis of the prototype $z_b$, perpendicular to the flapping movement plane. Based on previous works, the thrust force is considered as a function of the flapping frequency alone, and is computed in previous works [19], [21] as a linear function:

$$T = 2(c_1 f + c_2), \tag{5}$$

with $c_1$ and $c_2$ experimentally identified in [19].

However, there are different effects to consider for a FWMAV moving in forward flight. The incoming velocity provides an additional aerodynamic effect, modifying the resulting forces of the wings. If flapping movement is neglected, the aerodynamic forces can be expressed as lift $L$ and drag $D$, perpendicular and parallel to the incoming air. Then, we can compute the dimensionless aerodynamic coefficients $C_L$ and $C_D$ with the formulation from [22] for a flat plate at high angles of attack:

$$C_L = \frac{L}{\frac{1}{2}\rho S V^2} = \pi\sin(2\alpha), \tag{6}$$

$$C_D = \frac{D}{\frac{1}{2}\rho S V^2} = 0.69 - \cos(2\alpha), \tag{7}$$

with $\rho$ the air density, considered constant at sea level, $S$ the wing surface, and $V$ the flight velocity which has been defined in terms of the state variables in section II-A, as well as the angle of attack $\alpha$.

The Strouhal number based on the flapping amplitude is the non-dimensional term that relates the effects of the flapping movement and the incoming velocity ($St = fh_0/U$, with $h_0$ the flapping amplitude). When this number is below 0.1, the aerodynamics can be considered quasi-steady. For the range 0.2-0.6, the movement is in the unsteady aerodynamics [23]. For our case, the number is in the range of 1-2. Then, the effects are in the same order. The solution proposed here is to consider the resultant forces as a sum of both effects, considering the thrust of the flapping wings and the lift and drag generated by the forward flight. Note that in the hovering case the aerodynamic forces due to the forward velocity become 0, so the formulation would also be valid. However, at higher pitch angles and faster velocities, the unsteady aerodynamic effects of flapping wings in forward flight become more important (see [24]) and the model would start to fail.

Note that flexibility has not been considered as the deformations with the forces in forward flight are quite lower than the deformations from the flapping movement. In fact, although the aerodynamic effects are in a similar order, the inertial forces of the flapping movement provide an additional deformation to the wing that is key for the resultant thrust force. Flexibility is not expected to play such an important role in forward flight aerodynamics, as will be proven in experiments.

Considering this, we can formulate the aerodynamic forces and moment in the body frame, given in terms of the angle of

**IEEE Robotics and Automation Letters (RA-L) paper, presented at ICRA 2026, Vienna, Austria. Cite as RA-L paper.**

attack:

$$X = D\sin(\alpha) + L\cos(\alpha), \tag{8}$$

$$Z = -T + D\cos(\alpha) - L\sin(\alpha), \tag{9}$$

$$M = Tl_d - D[l_d\cos(\alpha) + l_z\sin(\alpha)] + L[l_d\sin(\alpha) - l_z\cos(\alpha)], \tag{10}$$

where $l_z$ is the position of the aerodynamic center from the center of gravity in the $z_b$ axis, which is fixed, and $l_d$ is the deflection for pitch actuation (see figure 2), measured with the distance in the $x_b$ axis. With this formulation, we can define the equilibrium state of the FWMAV.

## III. Equilibrium state

For the equilibrium state, the derivatives of the state variables are 0. Then we have 3 state variables to be defined $(u, w, \theta)$ with two control variables ($l_d$ and $f$, or alternatively $T$). However, if we define an additional restriction, the thrust will be fixed and we can obtain the state as a function of the deflection of the pitch actuation $l_d$. In this case, the equilibrium state will be solved for a horizontal flight.

### A. Angle Transformation

Once the horizontal flight case is imposed, the angle of attack can be written as a function of the pitch angle in wind still environments. Note that there are two cases. If the pitch is negative, the angle of attack will be also negative as observed in figure 2 and the FWMAV will move forward. On the other hand, if the pitch is positive, the angle of attack will also be positive and the FWMAV will move backward. The relation between the angle of attack and the pitch angle in both cases is defined by:

$$0 \leq \theta \leq 90 \rightarrow \alpha = \frac{\pi}{2} - \theta; \tag{11}$$

$$-90 < \theta < 0 \rightarrow \alpha = -\frac{\pi}{2} - \theta. \tag{12}$$

The transformation of the angles is similar in both cases. However, the solution will be similar in both cases, with the opposite direction, even though the formulation is different. The angle transformations are derived here for both cases. First, equations (8)-(10) are expressed in terms of $\alpha$, so they should be written in terms of $\theta$. For a positive pitch angle, we have:

$$\sin(\alpha) = \sin\left(\frac{\pi}{2} - \theta\right) = \cos(\theta), \tag{13}$$

$$\cos(\alpha) = \cos\left(\frac{\pi}{2} - \theta\right) = \sin(\theta), \tag{14}$$

and for the negative pitch angle,

$$\sin(\alpha) = \sin\left(-\frac{\pi}{2} - \theta\right) = -\cos(\theta), \tag{15}$$

$$\cos(\alpha) = \cos\left(-\frac{\pi}{2} - \theta\right) = -\sin(\theta). \tag{16}$$

Then, both the lift coefficient and the drag coefficient can also be written in terms of the pitch angle. For a positive pitch angle, the following formulation is obtained:

$$C_L = \pi\sin(2\alpha) = \pi\sin(\pi - 2\theta) = \pi\sin(2\theta), \tag{17}$$

$$C_D = 0.69 - \cos(2\alpha) = 0.69 + \cos(2\theta). \tag{18}$$

In this case, the final expression of both coefficients is the same for a negative pitch angle as $(\pi - 2\theta) = (-\pi - 2\theta)$.

### B. Derivation of Equilibrium State

Here the analysis is written for the case of a positive pitch angle, obtaining the following system of equations:

$$0 = (L - mg)\sin(\theta) + D\cos(\theta), \tag{19}$$

$$0 = (mg - L)\cos(\theta) + D\sin(\theta) - T, \tag{20}$$

$$0 = Tl_d - D[l_d\sin(\theta) + l_z\cos(\theta)] + L[l_d\cos(\theta) - l_z\sin(\theta)]. \tag{21}$$

The equation for the forces in both axes can be simplified using the inertial reference frame:

$$mg = T\cos(\theta) + L, \tag{22}$$

$$0 = T\sin(\theta) - D. \tag{23}$$

From equation (23) we can substitute the thrust in equation (21), obtaining

$$0 = -D\left[l_d\left(\sin(\theta) - \frac{1}{\sin(\theta)}\right) + l_z\cos(\theta)\right] + L[l_d\cos(\theta) - l_z\sin(\theta)], \tag{24}$$

and with a further simplification, we obtain

$$0 = \left[\frac{D}{\tan(\theta)} + L\right][l_d\cos(\theta) - l_z\sin(\theta)]. \tag{25}$$

Note that both drag and lift forces are positive magnitudes in this case. Therefore, to obtain a solution to the equation the second term has to be zero, providing an explicit formulation of the equilibrium pitch angle as a function of the deflection of the pitch actuation,

$$\tan(\theta) = \frac{l_d}{l_z}. \tag{26}$$

In the case of a negative pitch, the tangent would be negative, but also the lift from equation (17), so the solution is the same. This result is independent of the formulation for the lift and drag coefficients, so it would be valid also for an experimental identification of those coefficients. Additionally, if we had considered a negative pitch angle, the same solution would have been obtained, proving that a negative deflection of the pitch actuation would lead to a negative pitch angle. The velocity can also be obtained explicitly from equation (22), substituting the thrust with equation (23),

$$V = \sqrt{\frac{2mg}{\rho S\left[\frac{C_D}{\tan(\theta)} + C_L\right]}}. \tag{27}$$

We see that, to obtain the velocity in the equilibrium state, we need the explicit formulation of the aerodynamics lift and drag coefficients. Therefore, the correct formulation of the forces leads to a more accurate estimation of the range of velocities during the design of the FWMAV. Once the velocity and the pitch angle are known, the thrust force is obtained from equation (23):

$$T = D/\sin(\theta). \tag{28}$$

**IEEE Robotics and Automation Letters (RA-L) paper, presented at ICRA 2026, Vienna, Austria. Cite as RA-L paper.**

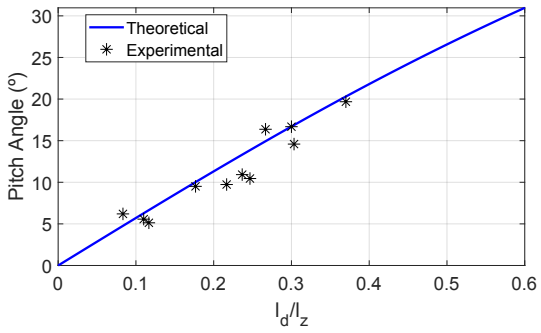


Fig. 3. Pitch angle as a function of the actuator deflection with experimental comparison. $l_d$ is defined with a transformation from the servomotor signal measured physically, and $l_z$ is measured with the center of gravity position and the wing center of pressure, placed at a 50% of the chord from the leading edge [22].

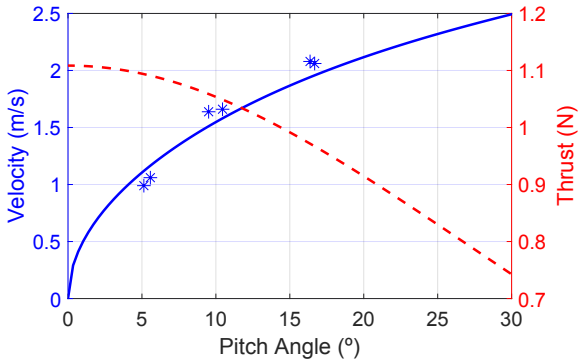


Fig. 4. Equilibrium state for the velocity and thrust required for maintaining a constant altitude as a function of the pitch angle. Stars refer to experimental values of the velocity.

And, consequently, the frequency can be obtained from equation (5) providing the necessary control actuation for maintaining the height during flight.

## IV. Results

A Flapper Nimble+ [21] has been used for the experimental validation, flying into the CyberZoo arena, the indoor flight zone at TU Delft. The pitch angle is estimated on board with an IMU [25]. The experiments are performed as follows. First, the FWMAV takes off and keeps a hovering state during 5 s. Then, a certain pitch angle is commanded, keeping the height and the yaw angle with no roll for the flight distance of the CyberZoo. Simulation and analytical results have been obtained with the specific characteristics of this FWMAV.

Open loop flight with the Flapper Nimble+ is unstable, so a cascade PD controller is active during flight for the pitch angle and the height. The experiments are performed with the default parameters of the Flapper Nimble+, that can be consulted online[1]. As further commented in subsection IV-B, the controller does not correct the permanent error in the pitch angle as it has no integral term. Therefore, the commanded pitch attitudes $[10^o, 20^o, 30^o]$ are not reached, and the Flapper stabilizes at lower pitch angles. There are results from 11 flights, at least 3 flights for each commanded pitch, one for a reference pitch of $40^o$, for which the limited space provides less flight time and therefore less reliability of the results. The height is estimated in all flights, but only some of them have estimations for the horizontal positions, so there are only reduced data on the flight velocity. The height controller maintains the altitude of the FWMAV, performing a horizontal flight as described in section III.

### A. Equilibrium State

The results of equations (26)-(28) are presented here to analyze how the FWMAV behaves in forward flight states. As the results are provided as decoupled equations, the implementation is simple.

[1]https://github.com/bitcraze/crazyflie-firmware

Figure 3 shows the experimental results for the pitch angle in the permanent state, compared to the analytical results for the equilibrium state. The deflection $l_d$ is calculated from the PWM signal to the pitch servomotor, with a transformation to obtain the position of the center of pressure. Note that most experiments reach a permanent pitch angle close to the analytical prediction. The values are obtained with an average pitch angle and pitch actuator deflection for each flight, after 1 s for stabilization. The dynamics provide the time of the transient phase and will be explained in more detail in Subsection IV-B. Flight time varies for each experiment due to the limited space. The average pitch angle and pitch actuator deflection are computed for the stabilized flight conditions (see section IV-B), during variables time lapses (from 3 s to 1.5 s). For the highest values of the pitch angle, the velocity is higher and there is a shorter flight time, providing higher uncertainty in the results. In addition, there are perturbations during flights that add uncertainty to the results, with standard deviations around $4^o$ for low pitch angles and up to $8^o$ for the higher pitch angles. Longer flight times are needed to obtain more reliable values (and, therefore, larger flight areas).

Some of the flights also included velocity data from motion capture system, validated with the analytical curve in figure 4. Note again how the results for the lowest pitch angles ($\theta \sim$ 5-10) have less uncertainty for different flights, while for the highest pitch angles the differences are higher between experiments. The trend for the velocity curve with the pitch angle agrees quite well with the analytical curve. The thrust curve, also plotted in figure 4, has not been validated as it depends on the battery charge state and these data were not recorded.

Note also from the analytical results in figure 3 that the relation between the pitch angle and the deflection is almost linear for low pitch angles. In fact, from equation (26), the linear approximation can be obtained for the pitch angle, $\theta \approx l_d/l_z$ for $\theta \ll 1$, which is valid for the experiments performed from figure 3. Note also the influence of the design parameter $l_z$. If this distance is small, the range of pitch angles for level flight will be wider.

Analytical results for velocity and thrust also provide useful insights into the forward movement of the flapper. For exam-

**IEEE Robotics and Automation Letters (RA-L) paper, presented at ICRA 2026, Vienna, Austria. Cite as RA-L paper.**

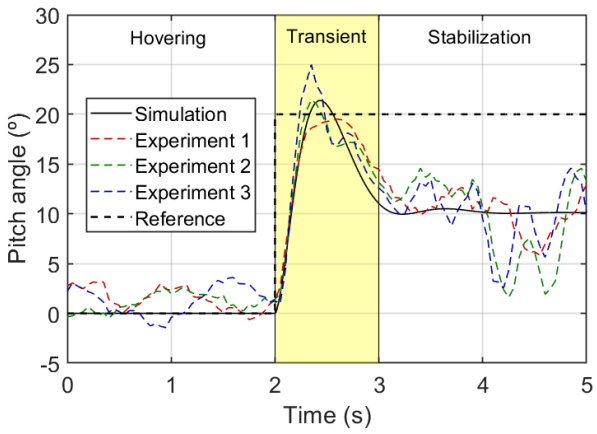


Fig. 5. Evolution of the pitch angle for a step pitch control signal of $20^o$.

ple, figure 4 shows how the velocity increases rapidly at lower pitch angles but the slope decreases with a pitch angle of $10^o$. Due to the low weight of the FWMAV, it needs to reach very high pitch angles to have a high velocity in steady horizontal flight. Increasing the thrust to get faster, would result in a climbing flight state. However, the range of the actuator is a limit for the pitch angle and, therefore, for the maximum velocity in horizontal flight. The analytical velocity is obtained using equations (6)-(7) for the aerodynamic force. Note that, although the formula used for the pitch angle was independent of the aerodynamic forces, the results for the velocity depend on the accuracy of the aerodynamic model.

There are also interesting details from the thrust in figure 4. Note how the thrust needed to maintain the flight altitude gets lower at higher pitch angles. This result agrees with the experimental observation in [4]. This is because the lift generation provided by the incoming velocity opposes the weight of the FWMAV, reducing the necessity of the flapping wing thrust. If the aerodynamic lift is not considered, the result would be opposite, predicting a higher thrust for maintaining altitude. The generation of drag due to the movement is not as important as the lift, as the drag coefficient in equation (18) decreases with the pitch angle, so the total thrust reduces significantly for pitch angles over $20^o$. However, if the pitch angle gets higher, the Strouhal number would decrease and the identified thrust force from equation (5) would lose validity, requiring alternative models for the predictions of aerodynamic forces.

### *B. Simulations*

To test the dynamic model, the system of non-linear equations (1)-(3) is implemented in MATLAB Simulink. Then, to add the real flight dynamics of the experiments, the original control architecture of the Flapper Nimble+ is included for both the pitch angle and the height. The yaw and roll controllers are neglected here as the lateral dynamics are not considered.

The pitch control of the flapper is performed through a cascade controller. The outer loop is a PD. The input is the pitch reference, and the output is the pitch rate. Then, this pitch rate is the input for a proportional controller which defines the PWM signal for the actuator. The dynamic response obtained for the pitch angle for a step in the reference from $0^o$ to $20^o$ is presented in figure 5, together with the experiments performed for that reference. Note the three separate phases. First, the FWMAV is in a hovering condition during 2 s. Then, when the reference is modified, there is a transient phase of 1 s, as commented before, where the pitch angle goes to a peak around $20^o$ and then it reduces to approximately $10^o$. This transient phase time agrees with the characteristic time of the dynamics derived in subsection II-A, quite slower than the characteristic time related to the flapping frequency. The third phase is the stabilization around the permanent flight state. This simulation was implemented with the default controllers of the Flapper Nimble+. In the stable phases, both for hovering and forward flight, the experiments show bigger oscillations than the simulations, probably due to small gusts or other perturbations not considered in the model. However, the transient phase is very similar for both the overshoot and the time for reaching the permanent state, showing the good alignment of the model with the real dynamics of the FWMAV.

As commented before, and seen in figure 5, the pitch controller has a permanent error. To correct it, two different strategies are compared here in simulations. The first solution is to add an integral term to the outer loop of the controller, so it becomes a PID controller which should eliminate the permanent error. The second approach is a feedforward control that includes the computation of the equilibrium state (eq. (26)) into the signal of the actuator, so the controller is centered around the particular equilibrium position in each case.

For the height control, the original architecture also includes a cascade controller, with two PIs. The height permanent error is corrected, even though the simulations show that the convergence to the equilibrium state is slow. We follow the same process as for the pitch control, adding the computation of the equilibrium state (eq. (28)) to the actuator output, in this case, the signal of the motors. Then, the integral part of the controller is not considered. Additionally, a derivative is added to the controller to reduce the effects of sudden changes in the reference.

Figure 6 shows the response of the system when a step in the reference pitch angle is applied. The FWMAV is in an initial hovering state and the reference for the pitch angle is modified to $10^o$. The reference value for the feedforward controller is modified progressively during 2 s, avoiding a sudden change in the trim point of the pitch controller. The controller parameters for the pitch angle are $k_P = 15$, $k_I = 15$, and $k_D = 15$. The derivative part of the controller has been increased to avoid an excessive overshoot. The transient of the pitch angle is significantly faster by adding the reference of the equilibrium state than with the integral term, going from approximately 6 s to around 3 s. Furthermore, the pitch angle reaches the reference with just a slight overshoot.

Those differences are even more significant for the height control. In the case of the PID controller, the height goes over the reference and slowly returns to the reference (note that $z$ is positive downwards as shown in figure 2). The transient

**IEEE Robotics and Automation Letters (RA-L) paper, presented at ICRA 2026, Vienna, Austria. Cite as RA-L paper.**

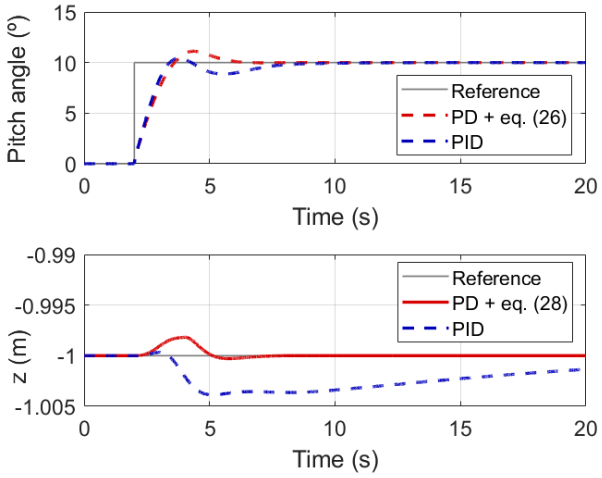


Fig. 6. Transient of the pitch angle and the height for a reference of $10^o$, comparing a PID controller (blue dashed line) and a PD controller with a feedforward term based on our equilibrium analysis (eq. (26) and (28)).

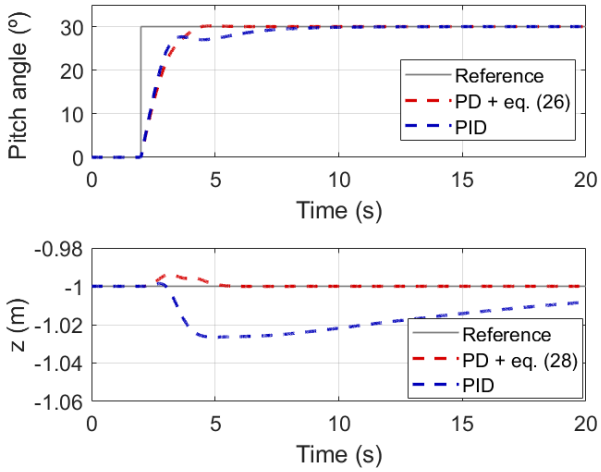


Fig. 7. Transient of the pitch angle and the height for a reference of $30^o$.

here takes more than 20 s, with an overshoot of near 0.5 cm. Both the transient time and the overshoot are reduced with the feedforward control. The transient time is reduced to approximately 3 s, with a slight deviation from the reference height, around 0.2 cm downwards, due to the transient of the pitch angle.

The same effect, but amplified, is observed in figure 7. The differences between both control strategies are similar, with the same transient time. However, now the overshoot in the pitch angle reduces to almost zero for the feedforward control. For the PID controller, the pitch angle is always under the reference, as the integral term takes longer to act than the proportional part, due to the difference in the actuator equilibrium point from the hovering state. For the height, there is a bigger overshoot for both cases, due to the bigger step in the pitch angle, but it is still much smaller for the feedforward control, less than 1 cm, than for the PID controller, around 2.5 cm.

Note that the control tests performed here just intend to show how the computation of the equilibrium state obtained in section III can improve the control of the FWMAV. A further analysis should be developed to improve the integration of the equations in the control actions. Furthermore, simulations adding noise to the state estimation showed perturbations as those found in the experiments in figure 5 in the stabilization phase, for both the original controllers and the first approach control actions included here. Those problems should be corrected for precise control of the FWMAV. To implement the proposed controller, feedback from pitch and height state would be needed, as well as pitch rate and vertical velocity. Then, an additional control effort would be needed for rejecting perturbations, avoiding the oscillations around the stabilized state shown in figure 5.

## V. Conclusion

This work provides an analysis of the equilibrium state for a FWMAV. Results improve state-of-the-art models by not focusing only on the dynamic response of the controllers and stability but also including information on the permanent regime equilibrium state.

The proposed basic dynamic model includes the definition of decoupled aerodynamic forces to define separately the thrust generated by the flapping movement and the lift and drag forces obtained by the incoming velocity when the flapper moves forward. The formulation for the coefficients was obtained from previous studies, but used here together to identify the effects of both forces. This formulation, developed for high Strouhal numbers and high angles of attack, provides a simple approximation for forward flight of tailless FWMAVs.

Given the dynamic model, the equilibrium state for leveled forward flight of tailless FWMAV is derived for the first time. The formulation presented is explicit in terms of the pitch actuation, obtaining decoupled analytical expressions for the pitch angle and the velocity, and providing an additional expression for the necessary thrust/frequency to perform horizontal flight, maintaining a constant height. In addition, the simplicity of the solutions makes it possible to include them in the controller design, eliminating permanent errors.

The analytical expression also shows a non-linear relation with the velocity. A linear approximation can be used for low pitch angles, losing validity as the pitch angle increases. For the thrust, results show how forward flight improves the efficiency of FWMAVs, reducing the necessary thrust to maintain the same height as the pitch angles become larger. Consequently, hovering is the least efficient state for a FWMAV, as observed in previous works [4].

The results are experimentally validated for pitch angle and velocity, showing good agreement even though the controller was not designed to reach the desired pitch angle. The results show how the model accurately predicts the equilibrium pitch angle and velocity for a range of the pitch angle between $0-30^o$. Limits of the validation for higher pitch angle should be analyzed in future work, but the model is expected to fail for lower Strouhal numbers. The validation is also extended to simulations of the dynamic response when a step in the

**IEEE Robotics and Automation Letters (RA-L) paper, presented at ICRA 2026, Vienna, Austria. Cite as RA-L paper.**

reference for the pitch angle moves the flapper from a hovering state to a forward flight state. The transient phase is perfectly characterized in the simulations, although the perturbations of real flights cause the FWMAV to be less stable once the permanent state is reached.

Some additional simulations are performed to compare the response of the system when the equilibrium state characterization is included with the performance of an added integral term for the pitch controller and the existing one for the height. Results show how taking into account the equilibrium state derived here significantly reduces the transient time. However, the overshoot is also slightly increased. Those simulations show how the formulation derived here can be used to improve the flight control of FWMAVs. However, this work is not focused on the development of control laws for tailless FWMAVs, and the simulations performed are just a basic approach to include our results to improve flight performance. Future work on the controller should include perturbation rejection to avoid the uncertainty in the flight state during stabilization phase, in order to implement the feedforward controller in real scenarios.

To achieve higher performance from the controllers, the equilibrium state formulation should be extended with a stability analysis, leading to a better understanding of the dynamic response of the FWMAV stable. Then, additional tests should be performed to analyze the stability under flight perturbations, as well as uncertainty and noise in the measures. Such future analysis would further enhance the modeling and control of FWMAVs.

## ACKNOWLEDGMENT

The authors acknowledge support from the Advanced Grant of the European Research Council GRIFFIN, Action 788247. Ernesto Sanchez-Laulhe acknowledges his predoctoral contract at the University of Malaga. The authors acknowledge the support of Agnieszka Nowak and Stein Stroobants in the experimental validation.

## REFERENCES

[1] M. Keennon, K. Klingebiel, and H. Won, "Development of the nano hummingbird: A tailless flapping wing micro air vehicle," in *50th AIAA aerospace sciences meeting including the new horizons forum and aerospace exposition*, p. 588, 2012.

[2] N. T. Jafferis, E. F. Helbling, M. Karpelson, and R. J. Wood, "Untethered flight of an insect-sized flapping-wing microscale aerial vehicle," *Nature*, vol. 570, no. 7762, pp. 491–495, 2019.

[3] H. V. Phan, S. Aurecianus, T. Kang, and H. C. Park, "Kubeetle-s: An insect-like, tailless, hover-capable robot that can fly with a low-torque control mechanism," *International Journal of Micro Air Vehicles*, vol. 11, p. 1756829319861371, 2019.

[4] M. Karásek, F. T. Muijres, C. De Wagter, B. D. Remes, and G. C. De Croon, "A tailless aerial robotic flapper reveals that flies use torque coupling in rapid banked turns," *Science*, vol. 361, no. 6407, pp. 1089–1094, 2018.

[5] G. de Croon, "Flapping wing drones show off their skills," *Science Robotics*, vol. 5, no. 44, p. eabd0233, 2020.

[6] Z. J. Wang, "Dissecting insect flight," *Annu. Rev. Fluid Mech.*, vol. 37, pp. 183–210, 2005.

[7] K. Y. Ma, P. Chirarattananon, S. B. Fuller, and R. J. Wood, "Controlled flight of a biologically inspired, insect-scale robot," *Science*, vol. 340, no. 6132, pp. 603–607, 2013.

[8] H. V. Phan, T. Kang, and H. C. Park, "Design and stable flight of a 21 g insect-like tailless flapping wing micro air vehicle with angular rates feedback control," *Bioinspiration & biomimetics*, vol. 12, no. 3, p. 036006, 2017.

[9] X. Zhang and H. Liu, "A three-axis pd control model for bumblebee hovering stabilization," *Journal of Bionic Engineering*, vol. 15, pp. 494–504, 2018.

[10] Z. Tu, F. Fei, J. Zhang, and X. Deng, "An at-scale tailless flapping-wing hummingbird robot. i. design, optimization, and experimental validation," *IEEE Transactions on Robotics*, vol. 36, no. 5, pp. 1511–1525, 2020.

[11] W. Siqi, S. Bifeng, C. Ang, F. Qiang, and C. Jin, "Modeling and flapping vibration suppression of a novel tailless flapping wing micro air vehicle," *Chinese Journal of Aeronautics*, vol. 35, no. 3, pp. 309–328, 2022.

[12] X. Deng, L. Schenato, W. C. Wu, and S. S. Sastry, "Flapping flight for biomimetic robotic insects: Part i-system modeling," *IEEE Transactions on Robotics*, vol. 22, no. 4, pp. 776–788, 2006.

[13] J.-K. Kim and J.-H. Han, "A multibody approach for 6-dof flight dynamics and stability analysis of the hawkmoth manduca sexta," *Bioinspiration & biomimetics*, vol. 9, no. 1, p. 016011, 2014.

[14] G. K. Taylor and A. L. Thomas, "Dynamic flight stability in the desert locust schistocerca gregaria," *Journal of Experimental Biology*, vol. 206, no. 16, pp. 2803–2829, 2003.

[15] M. Sun, J. Wang, and Y. Xiong, "Dynamic flight stability of hovering insects," *Acta Mechanica Sinica*, vol. 23, no. 3, pp. 231–246, 2007.

[16] C. T. Orlowski and A. R. Girard, "Dynamics, stability, and control analyses of flapping wing micro-air vehicles," *Progress in Aerospace Sciences*, vol. 51, pp. 18–30, 2012.

[17] L. T. K. Au, V. H. Phan, and H. C. Park, "Longitudinal flight dynamic analysis on vertical takeoff of a tailless flapping-wing micro air vehicle," *Journal of Bionic Engineering*, vol. 15, pp. 283–297, 2018.

[18] T. Roelandt and D. Vandepitte, "Inherently stable descending flight of a tailless flapping wing micro air vehicle by upward wing elevation," *International Journal of Micro Air Vehicles*, vol. 15, p. 17568293231178263, 2023.

[19] K. M. Kajak, M. Karásek, Q. P. Chu, and G. De Croon, "A minimal longitudinal dynamic model of a tailless flapping wing robot for control design," *Bioinspiration & biomimetics*, vol. 14, no. 4, p. 046008, 2019.

[20] L. Ristroph, G. Ristroph, S. Morozova, A. J. Bergou, S. Chang, J. Guckenheimer, Z. J. Wang, and I. Cohen, "Active and passive stabilization of body pitch in insect flight," *Journal of The Royal Society Interface*, vol. 10, no. 85, p. 20130237, 2013.

[21] C. Wang, S. Wang, G. De Croon, and S. Hamaza, "Embodied airflow sensing for improved in-gust flight of flapping wing mavs," *Frontiers in Robotics and AI*, vol. 9, p. 1060933, 2022.

[22] Z. J. Wang, J. M. Birch, and M. H. Dickinson, "Unsteady forces and flows in low Reynolds number hovering flight: two-dimensional computations vs robotic wing experiments," *Journal of Experimental Biology*, vol. 207, pp. 449–460, 01 2004.

[23] D. Floryan, T. Van Buren, C. W. Rowley, and A. J. Smits, "Scaling the propulsive performance of heaving and pitching foils," *Journal of Fluid Mechanics*, vol. 822, pp. 386–397, 2017.

[24] E. Sanchez-Laulhe, R. Fernandez-Feria, and A. Ollero, "Simplified model for forward-flight transitions of a bio-inspired unmanned aerial vehicle," *Aerospace*, vol. 9, no. 10, p. 617, 2022.

[25] J. Verboom, S. Tijmons, C. De Wagter, B. Remes, R. Babuska, and G. C. de Croon, "Attitude and altitude estimation and control on board a flapping wing micro air vehicle," in *2015 IEEE International Conference on Robotics and Automation (ICRA)*, pp. 5846–5851, IEEE, 2015.